



An Integrated Analysis with Predictions on the Architecture of the τ Ceti Planetary System, Including a Habitable Zone Planet

Jeremy Dietrich¹  and Dániel Apai^{1,2} 

¹ Department of Astronomy, The University of Arizona, Tucson, AZ 85721, USA; jdietrich1@email.arizona.edu

² Lunar and Planetary Laboratory, The University of Arizona, Tucson, AZ 85721, USA

Received 2020 August 11; revised 2020 October 22; accepted 2020 October 26; published 2020 December 7

Abstract

τ Ceti is the closest single Sun-like star to the solar system and hosts a multiplanet system with four confirmed planets. The possible presence of additional planets, especially potentially habitable worlds, remains of great interest. We analyze the structure of the τ Ceti planetary system via the DYNAMITE algorithm, combining information from exoplanet population statistics and orbital dynamics with measurements of this specific system. We also expand DYNAMITE to incorporate radial velocity information. Our analysis suggests the presence of four additional planets, three of which match closely with the periods of three tentative planet candidates reported previously. We also predict at least one more planet candidate with an orbital period between ~ 270 and 470 days, in the habitable zone for τ Ceti. Based on the measured $m \sin i$ values of the confirmed planets, we also assess the possible masses and nature of the detected and undetected planets. The least massive planets and candidates are likely to be rocky, while the other planets and candidates could either be rocky or contain a significant gaseous envelope. The radial velocity observable signature from the predicted habitable zone planet candidate would likely be at or just above the noise level in current data, but should be detectable in future extremely high-precision radial velocity and direct-imaging studies.

Unified Astronomy Thesaurus concepts: Exoplanets (498); Astrostatistics (1882)

1. Introduction

As a lone G8V dwarf located 3.650 ± 0.002 pc from the Sun (e.g., Teixeira et al. 2009), τ Ceti has been extensively studied since the early 1900s. It is the second-closest star similar to our Sun after α Centauri A, and the closest single Sun-like star (e.g., Hall & Lockwood 2004). It was noted as early as 1916 that τ Ceti was a G dwarf with parallax of 320 mas (Adams 1916), an overestimate of only 17% from the current measured value. In the 1950s τ Ceti was theorized to be one of only two other stars within 5 pc of the Sun capable of supporting life in a hypothetical planetary system (Huang 1959), and therefore was targeted in Frank Drake’s Project Ozma with radio telescopes to search for repeated signals from advanced civilizations (Drake 1961). As planet hunting became more and more sophisticated, τ Ceti remained one of the favorite targets due to its similarity to our Sun.

Beyond (or possibly due to) its astronomical significance, τ Ceti is one of the few stars that plays important roles in popular culture. It has been prominently featured in science-fiction novels as a home to extraterrestrial civilizations by the likes of Isaac Asimov, Robert Heinlein, Ursula K. Le Guin, and Arthur C. Clarke. Multiple episodes of science-fiction TV show standards *Star Trek* and *Doctor Who* have referenced a planetary system with habitable worlds orbiting τ Ceti. All of these were created before any planets were discovered in the τ Ceti system.

Given its importance within and beyond astronomy, the planetary architecture of the τ Ceti system and its prospect for hosting a habitable world is of broad interest. As of yet, however, this nearby planetary system has only been partially explored. Thus, the question emerges: what other worlds may

be present in τ Ceti, where would these be located within the system, and would these planets be detectable?

The DYNAMITE³ (Dietrich & Apai 2020) algorithm can predict the presence and parameters of currently unknown planets in multiplanet systems. DYNAMITE combines specific—but often uncertain and incomplete—information on the given planetary system with robust, exoplanet population-level information and first-principles-based orbital dynamical considerations, an approach that can provide enhanced statistical understanding of individual planetary systems (see also Bixel & Apai 2017; Apai et al. 2018). This integrated approach was recently applied to over 40 Transiting Exoplanet Survey Satellite (TESS)-discovered multiplanet systems (Dietrich & Apai 2020). We will explore the τ Ceti system to assess contextual evidence for the presence of additional planets and guide searches for them. Furthermore, as the known planets e and f straddle the optimistic limits for the habitable zone around τ Ceti (e.g., Kopparapu et al. 2013), an integrative study can help statistical assessment of the presence of a potential habitable planet around the closest single Sun-like star.

This paper is organized as follows. Section 2 details the τ Ceti planetary system as well as its stellar properties, and we briefly introduce the assumptions in DYNAMITE used specifically for τ Ceti in Section 3. Section 4 presents the DYNAMITE predictions for the system. Finally, Section 5 discusses the effect of our assumptions on the results and the supporting statistical evidence for planet candidates reported, as well as exploring the nature of the planets (including their possible habitability) and assessing the predicted observational signatures for unknown candidates that can be tested in the near future.

³ <https://github.com/JeremyDietrich/dynamite>

Table 1
Stellar Parameters for τ Ceti

Parameter Name	Value	References
Spectral type	G8V	(a)
Mass (M_{\odot})	0.783 ± 0.003	(b)
Radius (R_{\odot})	0.793 ± 0.004	(b)
Luminosity (L_{\odot})	0.448 ± 0.010	(b), (c)
Temperature (K)	5344 ± 50	(c)
Distance (pc)	3.650 ± 0.002	(b)
Rotation period (days)	34	(d)
Age (Gyr)	5.8	(a)

Notes. (a) Mamajek & Hillenbrand (2008), (b) Teixeira et al. (2009), (c) Santos et al. (2004), and (d) Baliunas et al. (1996). The rotation period given by Baliunas et al. (1996) and the age given by Mamajek & Hillenbrand (2008) have no attached uncertainties. We do not report Gaia DR2 values for distance and radius, as those have higher uncertainties due to pixel saturation (Kervella et al. 2019).

2. The τ Ceti System

τ Ceti is a G-spectral type, main-sequence star that is somewhat smaller than the Sun and slightly less than half as luminous. It is also less active than the Sun, with not quite as strong a starspot cycle; observations of the rotation and activity cycle of τ Ceti argue for a nearly pole-on (i.e., low-inclination) configuration (e.g., Gray & Baliunas 1994). Relevant stellar parameters for τ Ceti can be found in Table 1, and the known system architecture (as stated in the following paragraphs) is shown in Figure 1.

Radial velocity (RV) data of τ Ceti collected over a decade contain multiple periodic signals with periods ranging from 14 to 630 days. The analyses of the periodic RV modulations argue for three unconfirmed planet candidates with periods of 14 (b), 35.4 (c), and 94.1 (d) days (Tuomi et al. 2013, hereafter T13) and four planets with periods of 20 (g), 49.4 (h), 163 (e), and 636 (f) days (T13; Feng et al. 2017; hereafter F17). In particular, F17 confirmed planets e and f and detailed two strong signals they attribute to planets g and h. However, while F17 did find marginal evidence for each of the planet candidates labeled b, c, and d in the study by T13, the signals were not strong enough to confirm these planets (see Table 2 for a summary of the known planet properties).

In addition to the RV-detected planets and planet candidates, there is also tentative evidence from astrometric measurements for the presence of an additional, long-period, very massive planet. A tangential velocity anomaly in the HIPPARCOS astrometric proper-motion measurements of τ Ceti can be interpreted as a Jovian-mass planet in a further out orbit ($1-2M_{\text{Jup}}$ at 3–20 au; Kervella et al. 2019). We do not include this candidate in our study, as the constraints on the planet candidate are too loose to meaningfully inform our analysis. However, we note that the inner edge of its semimajor axis range would be near a 4:1 period ratio with planet f, and would therefore provide an interesting region of period space to explore further.

τ Ceti is also known to host a debris disk, and its inclination was inferred to be $35^{\circ} \pm 10^{\circ}$ from the best-fit model to observations taken using the Herschel Space Observatory and the Atacama Large Millimeter Array (ALMA; Lawler et al. 2014; MacGregor et al. 2016). The comparison of the disk’s inferred inclination and the star’s inferred inclination suggest that the disk plane is in or close to the star’s equatorial plane.

This also implies that the planets in the system may too orbit at low-inclination orbits, seen nearly face-on from our vantage point.

3. Methods

In this study we use DYNAMITE to integrate the observational evidence on τ Ceti (considering its uncertainties and incompleteness) with statistical, population-level constraints on exoplanet populations (orbital period distributions, planetary architectures, planet size/mass distributions) and with orbital dynamical stability considerations. For a full description of DYNAMITE we refer to Dietrich & Apai (2020), and we only briefly review here the principles underpinning DYNAMITE.

The goal of DYNAMITE is to integrate the available specific and statistical information to predict the likelihood distributions for the orbital period, planet radius, and inclination for yet-undiscovered planets. DYNAMITE utilizes a Monte Carlo implementation. As detailed below, DYNAMITE draws from intrinsic planet size, orbital period, and inclination distributions, as established from the Kepler planet population statistics (e.g., Mulders et al. 2018). Putative planets drawn from these distributions are further analyzed for orbital stability: it has been shown (e.g., He et al. 2019) that long-term stability of pairwise planets in a system requires 8–10 mutual Hill radii separation. Therefore, we limit the orbital placements of planets to distances greater than 8 mutual Hill radii of each other. This is only an approximate necessary condition, and while it works for current populations, future studies could utilize a more precise formalism based on a fuller dynamical stability assessment (i.e., including nonpairwise or three-planet mutual interactions) of each manifestation of the system studied.

In the current implementation of DYNAMITE, we use two prescriptions for the planets’ orbital period probability distribution. In this study we explore and contrast these two currently equally valid prescriptions. The first prescription comes from the analysis of the Kepler planet population via the Exoplanet Population Observation Simulator (EPOS; Mulders et al. 2018). This study finds that planets are more likely to have similar period ratios between them, with each the period ratio being drawn from a Log-normal distribution. The second comes from the Exoplanets Systems Simulator (SysSim; He et al. 2019). This study finds that planets tend to be clustered in period space, with the probability of a specific period inside a cluster also determined by a Log-normal distribution.

The population statistics come from the Kepler data set, and DYNAMITE was tested on both Kepler and TESS multiplanet systems (for details, see Dietrich & Apai 2020), showing a high degree of accuracy in predicting the parameters. For transiting exoplanet systems, like those found by Kepler and TESS, the inclinations can be constrained via the transit impact parameter. In addition, planet radii are known from the transit depth and the stellar radius. In cases of nontransiting planets, however, where the planet radius is not known (i.e., for RV-detected exoplanets), we use the planet mass as a fundamental parameter instead of the planet radius. For these RV-detected systems, the planet mass is often degenerate with the orbital inclination unless another type of observation can constrain the system’s geometry.

The planets and planet candidates in the τ Ceti system have been identified via RV observations and, thus, in the following we will use planet mass as a fundamental parameter. While the

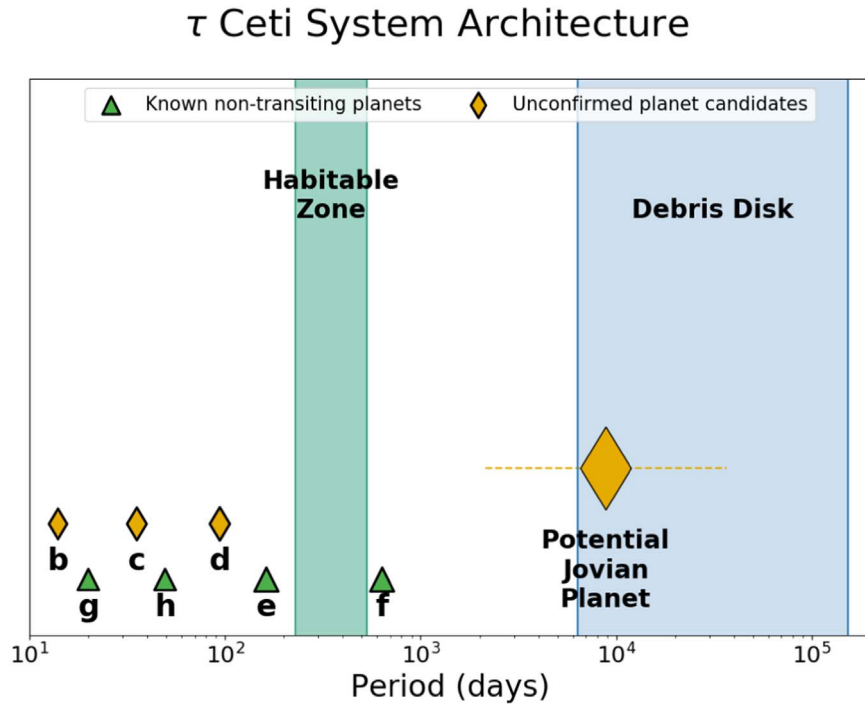


Figure 1. The τ Ceti system architecture, with known planets, unconfirmed planet candidates (with large error bars for the tentative Jovian planet detection), and the extents of the habitable zone and the debris disk. Relative marker sizes match planet sizes.

earlier study by T13 identified five planets (b, c, d, e, and f), the subsequent and more comprehensive follow-up study by F17 did not unequivocally confirm three of these (b, c, d). Therefore, in our study planets b, c, and d will be considered as planet candidates, and are not provided as priors to our DYNAMITE modeling. We do, however, use the robustly detected four planets (g, h, e, and f; Feng et al. 2017) as input.

We also assume that the planets are closely coplanar and that their orbital plane is aligned (within a few degrees) with the inclination of the debris disk itself. This assumption is reasonable as such planetary orbit and debris disk plane alignments have been reported for a number of systems (e.g., Apai et al. 2015; Plavchan et al. 2020), while—to our knowledge—no system with significant misalignment between debris disk and planetary orbital planes have been found. Under the assumption that the planetary orbits’ inclinations match that of the debris disk, the planets’ true masses would then be approximately 1.75 times the $m \sin i$ values measured via RV observations. We explore the effect of the assumption of relative coplanarity between the planets and the disk on the results of the analysis by testing a normal distribution for the debris disk inclination centered on the value from the best-fit model. We find that the above assumption only increases the width of the confidence interval for the predicted planet masses, but does not change the mean value. We also find that there would be no significant difference in the predicted planetary architecture with mutual inclinations between the planets and the disk $\lesssim 17^\circ$. If the planets had a lower inclination than the disk (more face-on), we find from our dynamical stability model that the closest planet and candidate pairs would become unstable at 17° less than the disk value. If the planets had a higher inclination than the disk (more edge-on), every planet and candidate would likely be rocky at inclinations 17° greater than the disk value. Therefore, we state that this assumption of relative coplanarity does not have a major

impact on the predicted planetary architecture of the τ Ceti system.

We use the possible masses of the known and predicted planets to constrain their nature and radii, via a mass–radius (M – R) relationship and by comparing their predicted mass/radii to such regimes as identified in the exoplanet population. As M – R relationships are not yet fully understood, in our study we compare results based on two M – R relationships: a nonparametric one and a power-law-based one. Specifically, we use the nonparametric M – R relationship of Ning et al. (2018) and the power-law M – R relationship characterized by Otegi et al. (2020), using both the rocky and volatile-rich populations. These two planet populations overlap between 5 and $25 M_\oplus$, so we test the predictions of both populations in that mass range separately. Notably, the predictions of their power-law relationships fit their entire data set within 2σ , and match well with ensemble results predicted from planet formation models (e.g., the Generation III Bern models; Emsenhuber et al. 2020a, 2020b).

4. Results

We report the properties of the planets and candidates, along with our predictions, in Table 2. The planet radii are not currently observable parameters for this system, as none of the planets transit and are too faint and/or too close to the host star for current direct-imaging techniques. Therefore, we report planet $m \sin i$ values determined from the planet radius distribution. We report results from our analysis based on different assumptions on the two different orbital period distributions and on three different M – R relationships. We find that the results from the two orbital period distributions are very similar and—for most planets—the derived planetary natures under the three different M – R relationships are similar too.

Table 2
 τ Ceti Planet and Planet Candidate Parameters

Name	Period (days)	$m \sin i$	Planet Type	Note	Origin/Reference
PxP-1	12.0 [7.10, 13.9]	2.0 ± 0.8	sub-Neptune	Equivalent to b?	Period ratio, NP
	14.0 [10.0, 14.8]		super-Earth		Period ratio, “rocky”
			super-Earth		Period ratio, “volatile”
			sub-Neptune		Clustered periods, NP
			super-Earth		Clustered periods, “rocky”
			super-Earth		Clustered periods, “volatile”
τ Ceti b	$14.0^{+0.017}_{-0.024}$	2.0 ± 0.8	Likely rocky	Unconfirmed candidate	T13
τ Ceti g	$20.0^{+0.02}_{-0.01}$	$1.75^{+0.25}_{-0.40}$	Likely rocky	Planet	F17
PxP-2	31.4 [28.8, 35.1]	3.1 ± 1.4	sub-Neptune	Equivalent to c?	Period ratio, NP
			super-Earth		Period ratio, “rocky”
			sub-Neptune		Period ratio, “volatile”
	34.0 [28.0, 36.4]		sub-Neptune		Clustered periods, NP
			super-Earth		Clustered periods, “rocky”
			sub-Neptune		Clustered periods, “volatile”
τ Ceti c	$35.4^{+0.088}_{-0.106}$	3.1 ± 1.4	Unknown	Unconfirmed candidate	T13
τ Ceti h	$49.4^{+0.08}_{-0.10}$	$1.83^{+0.68}_{-0.26}$	Likely rocky	Planet	F17
PxP-3	89.7 [78.7, 105]	3.6 ± 1.7	sub-Neptune	Equivalent to d?	Period ratio, NP
			super-Earth		Period ratio, “rocky”
			sub-Neptune		Period ratio, “volatile”
	67.0 [67.0, 103]		sub-Neptune		Clustered periods, NP
			super-Earth		Clustered periods, “rocky”
			sub-Neptune		Clustered periods, “volatile”
τ Ceti d	94.1 ± 0.7	3.6 ± 1.7	Unknown	Unconfirmed candidate	T13
τ Ceti e	$163^{+1.08}_{-0.460}$	$3.93^{+0.83}_{-0.64}$	Unknown	Planet	T13, F17
PxP-4	322 [277, 395]	$3.6 [2.70, 3.97]$	sub-Neptune	No equivalence	Period ratio, NP
		$1.91 [0.912, 6.14]$	super-Earth		Period ratio, “rocky”
		$1.91 [0.941, 3.37]$	super-Earth		Period ratio, “volatile”
	468 [406, 468]	$3.6 [2.70, 3.97]$	sub-Neptune		Clustered periods, NP
		$1.91 [0.912, 6.14]$	super-Earth		Clustered periods, “rocky”
		$1.91 [0.941, 3.37]$	super-Earth		Clustered periods, “volatile”
τ Ceti f	$636^{+11.7}_{-47.7}$	$3.93^{+1.05}_{-1.37}$	Unknown	Planet	T13, F17

Notes. *Name:* the given planet designations for both the confirmed planets and the candidates, as well as the planets we predict. PxP stands for predicted exoplanet. *Period:* the orbital period and uncertainty for the known planets and candidates, compared to our predicted value and 16%–84% confidence interval from DYNAMITE. *$m \sin i$:* the minimum mass of the planets, candidates, and predictions, not assuming an inclination. For PxP-1-3, we give the $m \sin i$ as the same value of the equivalent known planet candidate. *Planet type:* the predicted planet type for the PxPs and the natures for the known planets, all assuming an orbital inclination of 35° . *Note:* provides comparison between PxPs and known planets/candidates. *Origin/reference:* provides the reference paper for the confirmed planets and candidates, and the specific population models in DYNAMITE. NP is the nonparametric M - R relationship from Ning et al. (2018), rocky and volatile are the rocky and volatile-rich populations in the Otegi et al. (2020) power-law M - R relationship. Each line in the table for each PxP corresponds to a different combination of population models, and repeated values are combined together.

4.1. Period Distribution for Equal Period Ratios

Under the assumption that planets are found with equal period ratios between them, the DYNAMITE predictions agree very well with the combined picture from the analyses by T13 and F17. Specifically, DYNAMITE predicts four planet candidates (PxP-1 through PxP-4, see Table 2) with orbital periods at the relative likelihood maxima of 12.0, 31.4, 89.7, and 322 days. We point out that the planet candidates b, c, and d reported by T13 (which were not part of the DYNAMITE input) have very similar periods ($b = 14.0$ days, $c = 35.4$ days, and $d = 94.1$ days) to the predicted planets PxP-1, PxP-2, and PxP-3. Combining the four planets from F17 with the three unconfirmed (but now supported) candidates and the prediction of PxP-4 (which has no current equivalent candidate in the observational literature), the τ Ceti system becomes strongly dynamically packed. The relative likelihood in log-period space for the period ratio prescription is shown in the top of Figure 2.

4.2. Period Distribution for Clustered Periods

Under the assumption that the planets are clustered in period space, DYNAMITE also finds a very similar configuration to that described previously. Specifically, there are still four relative likelihood maxima for the predicted planets (again named PxP-1 through PxP-4 here) at periods of 14, 34, 67, and 468 days. These predictions are even closer (in orbital period) for PxP-1 and PxP-2 to planet candidates b and c, but farther away for PxP-3 to planet candidate d. The cluster assumption means DYNAMITE finds planet f in a second cluster in period space, away from the main cluster containing the other planets. Thus, DYNAMITE predicts the planet as close to the center of that cluster (and therefore as close to planet f) as possible (i.e., dynamically stable). The relative likelihood for the predicted planets in log-period space, under the clustered periods prescription, is shown in the bottom of Figure 2.

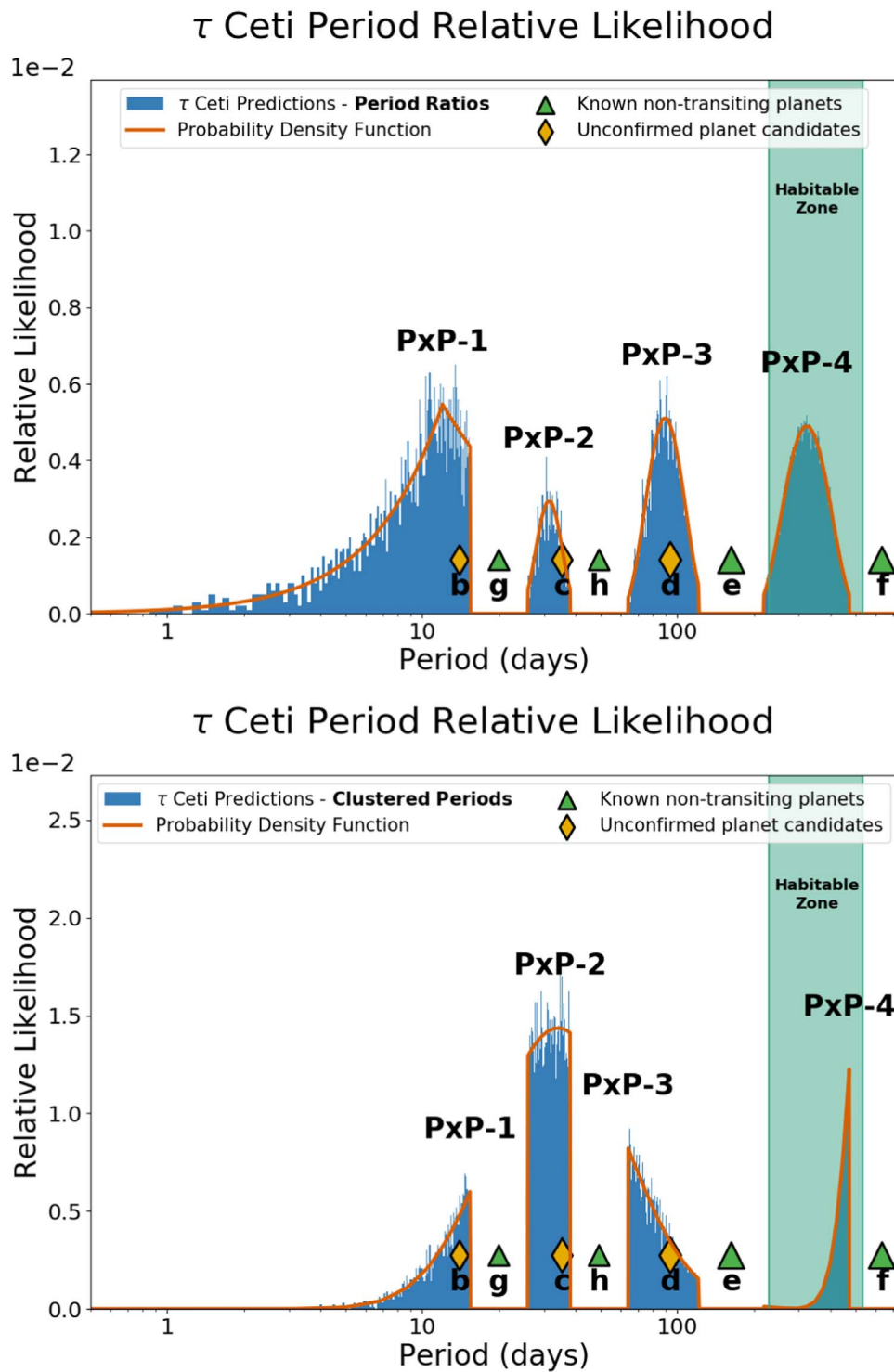


Figure 2. DYNAMITE predictions for the presence of hidden planets around τ Ceti in log-period space using the period ratio prescription (top) and clustered periods prescription (bottom).

4.3. Mass–Radius Relationships

On the basis of the DYNAMITE predictions we will now explore the possible ranges in mass and radius for the planets, planet candidates, and predicted planets in the τ Ceti system. We will follow three steps: first, we derive the likely mass distributions of the planets. Second, combining these with planet radius–mass relationships and planet occurrence rates (expressed in planet radii) we derive the likely distributions of

planet radii and masses in the system. Third—Section 4.4—we will use the derived M – R probability distributions to identify the possible natures of the planets, also considering the impact of key assumptions on the results. In the discussions in this and the following subsection, we also consider the uncertainties in the measurements as well as the sensitivity of the final results to key assumptions. The most important assumption is the adopted M – R relationship; therefore, we present and contrast

results assuming three different M – R relationships, which are representative to the state of the art.

For our first step—deriving the probability distribution functions of the planet masses—we start our analysis from the $m \sin(i)$ values observed for the confirmed planets and combine these with a constraint on the orbital inclinations to derive the likely true masses of the planets. The planetary orbital inclinations are not directly measured, but—as explained in Section 3—there are very strong astrophysical reasons to assume that the planetary orbits are overall well-aligned with the debris disk, for which good geometrical constraints exist from spatially resolved ALMA observations. With this constraint on the orbital inclinations, we find that all planets and planet candidates in the inner system likely fall between 3 and $7 M_{\oplus}$ in mass. Table 2 shows the derived planet mass ranges and inclinations.

A key assumption in the second step of our analysis is the M – R relationship adopted for smaller planets, of which multiple somewhat different variants have been proposed in the literature (e.g., Bashi et al. 2017; Chen & Kipping 2017; Ning et al. 2018; Otegi et al. 2020). Instead of adopting any single M – R relationship, we explore three different relationships, one from Ning et al. (2018) and two from Otegi et al. (2020). Therefore, our exploration of multiple M – R relationships quantifies the impact of this choice on the results. As one of our three relationships to explore, we chose the nonparametric relationship from Ning et al. (2018) as it provides a probabilistic measure of the mass and radius. This relationship conditions its predictions on the known mass/radius data we have gathered from exoplanet systems, where super-Earths/sub-Neptunes have the highest occurrence and therefore would be the most predictive. However, this conditionality also means there is not a 1:1 relationship between radius and mass, and it also greatly increases the computation time required for deriving mass distributions. Furthermore, as our second and third M – R relationships to explore, we adopted the two power-law relationships from Otegi et al. (2020) as these match data up to $120 M_{\oplus}$ very well. Based on these, we explore the difference between sub-Neptunes and super-Earths in a region of M – R space where these two planet populations overlap. This combined approach, therefore, also provides an assessment of the possible range of natures for these worlds.

We applied each M – R relationship to the known planet masses to find their radii, before—following Dietrich & Apai (2020)—we fit them to the Log-normal distribution for planet radius to find the best-fit distribution. We find that the known planet radii are close enough to each other to be statistically considered a single cluster in planet radius by DYNAMITE. The predicted planet radius distribution found from this best-fit of the four planets, for each of the three M – R relationships adopted, is shown in the left side of Figure 3. We then reversed the process and applied each M – R relationship on the radius distribution to get a distribution in planet masses, shown on the right side of Figure 3.

4.4. The Nature of Planets in the τ Ceti System

In this section we will build on the planet M – R probability distributions derived in Section 4.3 to explore the possible natures of the planets, i.e., by which broad categories they are most likely to fit (e.g., Earth/super-Earth/sub-Neptune/ice giants/evaporated cores). For our results on the natures of the planets, we simply refer to planet candidates b, c, and d also as

planets, as the derived natures would only be meaningful if the planets exist at all. In the following, we split the planets into two groups based on our mass predictions.

Planets b, g, and h. When using the nonparametric M – R relationship from Ning et al. (2018), these three planets would have likely been sub-Neptunes, with predicted radii above $2R_{\oplus}$ and a density consistent with a gaseous-volatile envelope. However, as these planets have expected masses of $5 M_{\oplus}$, when using both realizations of the power-law relationships from Otegi et al. (2020), these planets would be rocky planets, with radii less than $1.5 R_{\oplus}$. Therefore, we find that these worlds are either sub-Neptunes or rocky worlds, depending on which M – R relationships better capture reality.

Planets c–f. As with the previous planets, we find that the nonparametric M – R relationship from Ning et al. (2018) describes these four planets as sub-Neptunes. The planets have expected masses between 5.4 and $7 M_{\oplus}$, and therefore fall in the overlap region for the Otegi et al. (2020) power-law relationships. If predominantly rocky, these planets would have radii between 1.7 and $1.8 R_{\oplus}$ and would have approximately terrestrial density. These radii are close in size to the Fulton gap, a relative paucity of planets (Fulton et al. 2017), which may also separate primarily rocky worlds from those with significant gaseous envelopes. However, the data are also consistent with a different nature: under the volatile M – R relationship from Otegi et al. (2020), these planets would have planet radii between 2 and $2.4 R_{\oplus}$, and thus densities and nature comparable to the ice giants in our solar system.

When comparing the irradiation of the planets in the τ Ceti system to photoevaporation models (e.g., Owen & Wu 2017; Carrera et al. 2018), we find that the three innermost planets b, g, and c would likely have suffered from a significant degree of atmospheric loss due to photoevaporation. Therefore, if these planets had any gaseous envelopes, it is likely that these atmospheres would have evaporated and left behind a rocky core (Pascucci et al. 2019). However, for planet h and outwards, the radiative flux received from τ Ceti would not be strong enough to strip the envelope from the planet. Thus it is likely that if these planets had volatile-rich atmospheres, they would still retain them to this day.

5. Discussion

5.1. Support for Previously Identified Candidates b, c, and d

Based on RV measurements, T13 reported five planets in the τ Ceti system (labeled τ Ceti b–f). However, follow-up analysis by F17 found four planets in the system. They discovered new planets at 20 and 49 days (labeled τ Ceti g and h) and confirmed the presence of planets e and f at 163 and 636 days, but were not able to confirm the presence of planet candidates b–d at 14, 35, and 94 days. They found that the 14 day period signal becomes much less significant in later data sets when the 20 day signal is subtracted, and is, thus, attributed to stellar activity. Furthermore, the 35.4 day period signal was found to be much weaker than previously thought and close to the rotation period of the star. Finally, the 94 day period signal was noticeable but found in only a few of the data sets.

To assess the likelihood of planet candidates b–d in the system, we show that if planets were to be added within the orbit of planet e ($P \lesssim 162$ days), the periods for τ Ceti b–d are near the local maxima of the relative likelihood in period space. This is true for both exoplanet period distributions; the

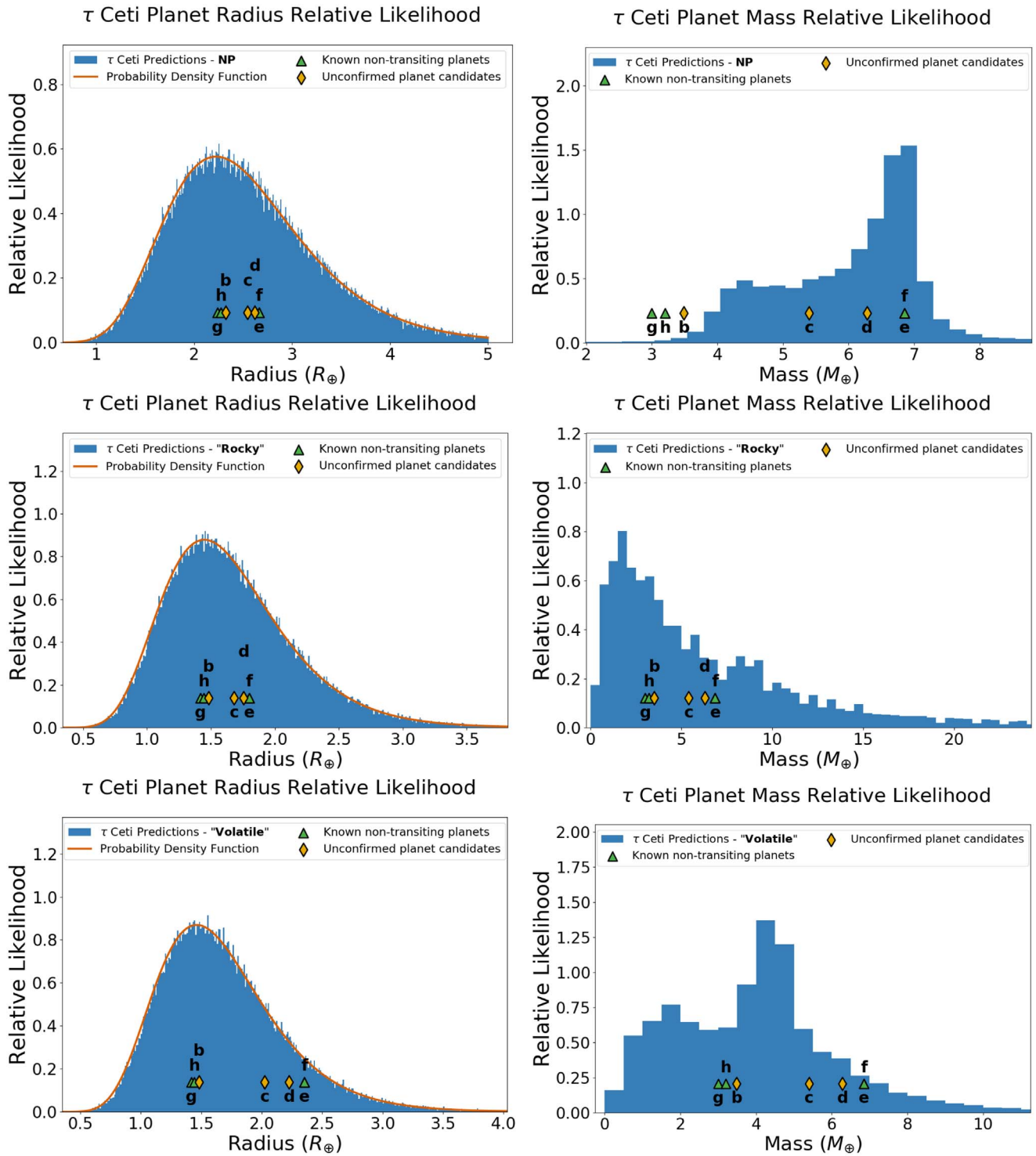


Figure 3. Left: planet radius histograms taken from the clustered radius model for three different $M-R$ relationships: Ning et al. (2018) nonparametric (NP; top), Otegi et al. (2020) power-law rocky (middle), and Otegi et al. (2020) power-law volatile (bottom). Right: planet mass histograms calculated from the radius histograms for the same three $M-R$ relationships.

clustered periods prescription is closer to the known signals for b and c, while the period ratio prescription is closer for d. Therefore, the predictions for planet candidates PxP-1, PxP-2, and PxP-3 provide contextual, statistical evidence that support the existence of planet candidates τ Ceti b-d, as does the dynamical stability analysis of the τ Ceti system. When only considering planets g, h, e, and f in the system, the average separation between each planet in units of mutual Hill radii is

~ 31.4 (assuming all planets orbit near the disk inclination). The peak in separation seen in population statistics is ~ 20 mutual Hill radii, with larger numbers (i.e., close to 40) indicating the presence of missing planets (e.g., Gilbert & Fabrycky 2020). Adding in τ Ceti b-d and PxP-4 with the period ratio description pushes the average separation down to ~ 15.6 Hill radii.

5.2. P_{xP-4} Characteristics—A Habitable Zone Super-Earth?

Both flavors of the orbital period distributions explored in our analysis result in the robust prediction that a planet in the habitable zone of τ Ceti is very likely. This prediction is, as discussed below, consistent with available data. T13 identify a possible ~ 315 day signal and performed extensive Keplerian modeling of the system both with and without that planet. They concluded that it was more likely an alias of the 168 day signal. F17 also found a relatively strong signal at ~ 318 days and concurred that it was an alias of their 162 day signal. However, due to the gap of factor ~ 4 in period space between planets e and f, DYNAMITE (and dynamically packing, in general) predicts another planet candidate, P_{xP-4}, in the period range between those two known planets.

With the four-planet architecture found by F17, under the clustered periods assumption, our analysis finds that planet f is separated from the other planets in period space and is in its own cluster. Therefore, we predict another planet as close to the center of that cluster (i.e., the period of planet f) as dynamically possible, near an orbital period of 468 days. In contrast, under the period ratio assumption, our analysis places the new planet with symmetric period ratios between itself and planets e and f, at a period of 322 days. Given the mass of τ Ceti as $0.783 M_{\odot}$, an orbital period of 322 days corresponds to an orbital semimajor axis of 0.848 au, and an orbital period of 468 days corresponds to orbital semimajor axis of 1.09 au. The conservative habitable zone for τ Ceti (effective temperature $T_{\text{eff}} = 5344$ K), as defined by Kopparapu et al. (2013) using their moist greenhouse and maximum greenhouse limits, lies between stellocentric distances of 0.703 and 1.26 au. Thus, P_{xP-4} would comfortably lie inside the habitable zone of τ Ceti.

As before, we explore the potential nature of P_{xP-4} by contrasting it to the exoplanet size–density trends. As explained below, we find that it may be a super-Earth, but could also be a volatile-rich sub-Neptune. We calculated the mass of the P_{xP-4} planet candidate by translating its predicted planet radius distribution into a mass distribution via our M – R relationship. This provided the predicted mass of $3.33 M_{\oplus}$ for the power-law relationships from Otegi et al. (2020) and $6.30 M_{\oplus}$ for the nonparametric M – R relationship from Ning et al. (2018). Planets of the former mass ($3.33 M_{\oplus}$) would likely always be rocky, as the lower limit for the volatile-rich population from Otegi et al. (2020) where anything below $5 M_{\oplus}$ is considered rocky. Under the rocky assumption, $1 M_{\oplus}$ lies at the 7th percentile of the planet mass distribution for the τ Ceti system. Planets with the latter mass ($M_p \approx 6$ – $7 M_{\oplus}$) would have planet radii $\sim 1.8 R_{\oplus}$ if they were rocky, but could also likely contain a gaseous envelope and have radii of 2.1 – $2.4 R_{\oplus}$.

5.3. Observational Signatures of P_{xP-4}

Our prediction of a habitable zone planet, P_{xP-4}, in the τ Ceti system raises the question of whether this planet could be detected. In this section we explore the observational signatures expected from this planet and discuss what measurements may clarify whether it is a habitable zone super-Earth or a—presumably uninhabitable—sub-Neptune. Specifically, we will discuss the possibility of detecting P_{xP-4} via transits, RV, and direct imaging. Our analysis assumes that the inclination of P_{xP-4} is aligned with the disk and other planets in the system to within a few degrees. This assumption would make it very

unlikely that P_{xP-4} is detectable via transit observations, leaving RV and direct imaging as the viable options for the next decades of observations.

To estimate the RV semi-amplitude, we assume that P_{xP-4}'s orbital eccentricity is low, as would be expected in a high-multiplicity system (e.g., Limbach & Turner 2015; Van Eylen et al. 2019). Given its value for $m \sin i$ of 3.3 – $6.3 M_{\oplus}$, the RV semi-amplitude of P_{xP-4} would be ~ 0.2 – 0.4 m s^{-1} , which is similar in magnitude to the signals detected from τ Ceti g and h. This value is at or just above the noise limit for τ Ceti on the High Accuracy Radial Velocity Planet Searcher (HARPS; Mayor et al. 2003) spectrograph, as characterized by F17. The Echelle SPectrograph for Rocky Exoplanets and Stable Spectroscopic Observations (ESPRESSO) spectrograph (Pepe et al. 2010) would likely be able to reach the required precision to detect P_{xP-4}, as it is able to reach $\sim 0.25 \text{ m s}^{-1}$ for Proxima Centauri (Suárez Mascareño et al. 2020), a fainter and more active star.

We will now explore τ Ceti's P_{xP-4} as a potential target for direct imaging. The relative proximity of τ Ceti to the solar system makes this system one of the premier targets for next-generation direct-imaging systems, both from space and from the ground. A direct-imaging detection of a potentially habitable P_{xP-4} would be revolutionary, as it could be exploited for a broad variety of follow-up efforts to characterize the planet in depth and to address a multitude of new science questions (for a community report, see Apai et al. 2017). At a distance of only 3.65 pc, the orbital semimajor axis of 0.848 au of P_{xP-4} corresponds to an angular separation of 250 mas, which is on par to recently imaged super-Jupiter exoplanets (e.g., Lagrange et al. 2010; Macintosh et al. 2015). Unlike the hot young super-Jupiters imaged with extreme adaptive systems, however, P_{xP-4} is neither young, hot, or massive, and thus poses an orders-of-magnitude greater contrast challenge than anything imaged as of now.

While imaging P_{xP-4} with current state-of-the-art facilities is not possible, the feat may be within grasp of future facilities. Thermal emission from P_{xP-4} should peak close to $\lambda_{\text{th}} = 10 \mu\text{m}$ due to the equilibrium temperature of this habitable zone planet. Current efforts for detecting a habitable zone Earth-sized planet around α Centauri through a 100 h-long integration with the Very Large Telescope's VISIR instrument show it is possible (e.g., Kasper et al. 2019). Although τ Ceti is at a distance 2.4 times greater than α Centauri, P_{xP-4} may be a factor of a few larger than Earth, somewhat countering the greater distance. Thus, while the intensity of P_{xP-4} may be detectable with the sensitivity of present-day, ultra-deep thermal infrared images (see also Wagner 2020), its relatively small projected separation (250 mas) falls within the contrast-limited region of such images, where sensitivity is greatly reduced (K. Wagner et al. 2020, in preparation). The next-generation large ground-based telescopes, such as the Giant Magellan Telescope (GMT),⁴ the Thirty Meter Telescope (TMT), or the European Extremely Large Telescope (E-ELT), should deliver increased thermal infrared sensitivity and a factor of several smaller inner working angles (e.g., Quanz 2015; Mazin et al. 2019; Wang et al. 2019), making direct detection of τ Ceti P_{xP-4} a promising possibility.

⁴ GMT Science Book, <https://www.gmto.org/sciencebook2018>.

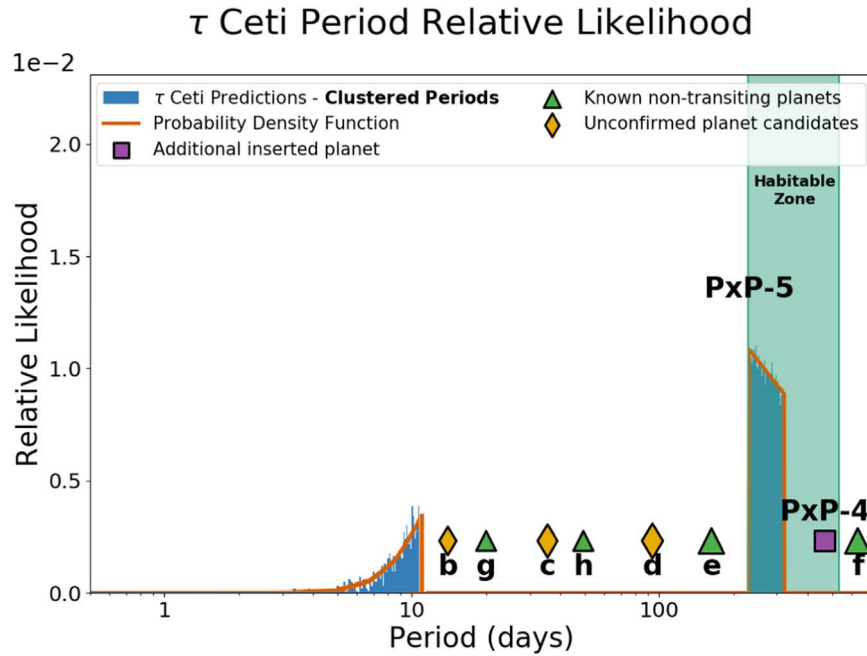


Figure 4. The clustered periods prescription predictions after adding in all four predicted exoplanets. The gap between e and the additional inserted planet Pxp-4 is large enough for another planet to fit in between, with a period of ~ 270 days, at the inner edge of the habitable zone.

Pxp-4 may also be detected in the future via reflected (scattered) light imaging. The brightness of the planet in scattered light depends on the physical separation from the host star, the Bond albedo, the scattering phase angle, and the illumination phase, which complicate the detection, identification, and interpretation of directly imaged habitable planets (e.g., Bixel & Apai 2020). It is likely that Pxp-4 would be $\sim 10^{-9}$ fainter than τ Ceti, requiring space-based, ultra-high-contrast imaging or interferometry to detect. Mission concepts that would be capable of detecting Pxp-4 have been proposed such as the Large UltraViolet Optical InfraRed Surveyor (LUVOIR; The LUVOIR Team 2019) the Habitable Exoplanet Observatory (HabEx; Gaudi et al. 2020), and the Large Interferometer For Exoplanets (LIFE; Quanz 2019), and may become operational within the next two decades.

Thus, we conclude that Pxp-4 is already likely detectable indirectly, via the RV modulations it imprints on its host star, and it will be directly detectable by the end of the current decade in thermal emission (with the extremely large ground-based telescopes), as well as an ideal target for space-based high-contrast imaging and spectroscopy in about two decades.

5.4. Habitable Planet in the τ Ceti System?

τ Ceti has long been a candidate to search for nearby life, and we find that the probability of having a rocky planet in the habitable zone is relatively high. The probability of additional planets to be sub-Neptunes with a gaseous/volatile envelope versus rocky super-Earths ranges from roughly equal to leaning toward rocky planets; across the $M-R$ relationships 50%–75% of injected planets had a planet mass below $5 M_{\oplus}$. However, the probability of finding specifically an Earth-like planet ($0.5 M_{\oplus} < M_p < 1.5 M_{\oplus}$) is low. The nonparametric $M-R$ relationship from Ning et al. (2018) had no significant probability of finding a planet with a mass between 0.5 and $1.5 M_{\oplus}$, whereas the rocky and volatile populations of the

power-law relationships from Otegi et al. (2020) had only $\sim 12\%$ and $\sim 3\%$, respectively, in that mass range.

A super-Earth planet in the habitable zone around τ Ceti would have an RV semi-amplitude of 0.4 m s^{-1} , which is above the noise floor of current spectrographs like HARPS and ESPRESSO. However, even across a decade of observations, this signal would still be difficult to find, especially due to the alias caused by Earth’s own orbital period. With even better extreme-precision RV (EPRV) measurements pushing down toward 1 cm s^{-1} precision, the ability to observe a signal from rocky planets in the habitable zone around τ Ceti will become much easier, and EPRV data would even be able to find an Earth-like planet (RV semi-amplitude $\lesssim 0.1 \text{ m s}^{-1}$) around τ Ceti.

The period ratio prescription has low probability of adding in an additional planet after inserting Pxp-1-3 at the values for the known planet candidates b–d and adding Pxp-4 at its relative likelihood maxima. These four predicted planets dynamically pack the system with relative period ratios for each pair of planets close to the Kepler statistical mean. The clustered periods prescription, after adding in Pxp-1-3 at the values for planet candidates b–d and Pxp-4 at its relative likelihood maxima, also allows for an additional planet candidate to be placed at ~ 270 days, corresponding to an orbital semimajor axis of 0.754 au. This hypothetical planet, too, would be within the habitable zone assuming an inner limit of 0.703 au. This additional prediction from the clustered periods prescription is favorable as it fits the system parameters well. The integrated likelihood of the second injection is higher than the first injection, and the overall average planet separation in units of mutual Hill radii for the nine planet system prediction via the clustered periods prescription is 15.5. This is very similar to the eight-planet system prediction via the period ratio prescription of 15.6. The new injection test, after adding in the eight current candidates, is shown in Figure 4.

6. Summary

We applied the DYNAMITE algorithm to provide an integrative analysis of the τ Ceti system, the second-closest Sun-like star to the solar system. The key findings of our study are as follows.

- (1) Using both orbital period distribution models, our analysis suggests that the three planet candidates (b, c, and d) reported by T13 at periods of ~ 14.0 , 35.4, and 94.1 days are likely to be real. These planets would dynamically pack the system and follow the Kepler population statistic for the first planet being found at an orbital period mode of 12 days (Mulders et al. 2018).
- (2) Our analysis predicts an additional, fourth planet candidate (PxP-4) at $P = 322$ days (when using the period ratio prescription) or at $P = 468$ days (using the clustered periods prescription). The period ratio prediction would fully pack the system out to known planet f, and matches a possible signal in the RV data seen by both T13 and F17 at 315–320 days. The clustered periods prediction also allows for another planet candidate between planet e and PxP-4.
- (3) Given the assumption that the orbital plane of the planets matches the visible debris disk at 35° , the planets and planet candidates are all super-Earths or sub-Neptunes ($3\text{--}7M_\oplus$). Similarly, we predict candidate PxP-4 to have a planet mass between 3.3 and $6.3 M_\oplus$. The probability that this candidate is rocky ($M_p < 5M_\oplus$) is more than 50%, but the likelihood of it being Earth-like ($0.5M_\oplus < M_p < 1.5M_\oplus$) is $\lesssim 10\%$.
- (4) With τ Ceti being Sun-like but only half as luminous, if PxP-4 orbits τ Ceti with a 320–470 day period (or an orbital semimajor axis of $\sim 0.85\text{--}1.09$ au), it would receive roughly 35%–60% of the light that Earth does. Thus, PxP-4 would straddle the center of τ Ceti's habitable zone (Kopparapu et al. 2013).
- (5) The low end of the predicted mass range for PxP-4 is near the masses of τ Ceti g–h and PxP-2/planet b ($3\text{--}3.5M_\oplus$). The high end of the predicted mass range for PxP-4 is near the masses of τ Ceti e–f ($\sim 7M_\oplus$) and similar to the mass of PxP-3 (a close match to the unconfirmed planet candidate d). Planets g and h, and planet candidate b are likely rocky, while planets e and f, along with planet candidates c and d, each have a roughly equal likelihood of being rocky or containing a significant gaseous envelope.
- (6) The predicted presence of PxP-4 in the habitable zone should be soon testable. While the RV semi-amplitude for PxP-4 of $0.2\text{--}0.4 \text{ m s}^{-1}$ is at the precision limit for τ Ceti of the current data, PxP-4 is likely to be within reach of the newest and near-future EPRV instruments. With the new generation of extremely large telescopes (GMT, TMT, and E-ELT), high-contrast thermal infrared imaging should enable direct detection and study of this world. Furthermore, this potentially habitable planet could be studied in great detail with future space-based telescopes, such as the mission concepts LUVOIR, HabEx, or LIFE.
- (7) If PxP-4 is close to the widest predicted orbits (i.e., has a period close to ~ 470 days), we find that an additional planet may reside in the habitable zone. This second

habitable zone planet would then have a period of ~ 270 days.

Our study demonstrates an approach to exploring the inner planetary systems of nearby stars. We combine uncertain and incomplete but specific information on planetary systems with robust statistical understanding of exoplanet population demographics and first-principles-based constraints on planetary dynamics. The current DYNAMITE implementation is computationally inexpensive and can be applied to a large sample of systems. The analysis done in this work and as carried out by Dietrich & Apai (2020) on the TESS sample of multiplanet systems takes a couple of minutes per system on a 16-core desktop computer, for every setup with the exception of the nonparametric model from Ning et al. (2018) as stated in Section 4.4. For the τ Ceti system, the integrated analysis supports the veracity of three planet candidates reported in the literature and predicts the presence of a habitable zone, possibly rocky planet (PxP-4). Soon, improved RV coverage should be able to directly test the predictions made in this study and possibly confirm the presence of PxP-4 in the habitable zone. This measurement will represent a great leap into clarifying the potential of the second-closest Sun-like star and closest single Sun-like star—an obvious target for biosignature searches—for hosting a habitable world.

We acknowledge support from the Earths in Other Solar Systems Project (EOS), grant No. 3013511 sponsored by NASA. The results reported herein benefited from collaborations and/or information exchange within NASA's Nexus for Exoplanet System Science (NExSS) research coordination network sponsored by NASA's Science Mission Directorate. We acknowledge use of the software packages NumPy (Harris et al. 2020), SciPy (Virtanen et al. 2020), Matplotlib (Hunter 2007), and MRExo (Kanodia et al. 2019). This paper includes data collected by the Kepler mission. Funding for the Kepler mission is provided by the NASA Science Mission Directorate. The citations in this paper have made use of NASA's Astrophysics Data System Bibliographic Services.

ORCID iDs

Jeremy Dietrich  <https://orcid.org/0000-0001-6320-7410>
 Dániel Apai  <https://orcid.org/0000-0003-3714-5855>

References

- Adams, W. S. 1916, *PASP*, **28**, 279
 Apai, D., Ciesla, F., Mulders, G. D., et al. 2018, arXiv:1803.08682
 Apai, D., Cowan, N., Kopparapu, R., et al. 2017, arXiv:1708.02821
 Apai, D., Schneider, G., Grady, C. A., et al. 2015, *ApJ*, **800**, 136
 Baliunas, S., Sokoloff, D., & Soon, W. 1996, *ApJL*, **457**, L99
 Bashi, D., Helled, R., Zucker, S., & Mordasini, C. 2017, *A&A*, **604**, A83
 Bixel, A., & Apai, D. 2017, *ApJL*, **836**, L31
 Bixel, A., & Apai, D. 2020, *AJ*, **159**, 3
 Carrera, D., Ford, E. B., Izidoro, A., et al. 2018, *ApJ*, **866**, 104
 Chen, J., & Kipping, D. 2017, *ApJ*, **834**, 17
 Dietrich, J., & Apai, D. 2020, *AJ*, **160**, 107
 Drake, F. D. 1961, *PhT*, **14**, 40
 Emshenhuber, A., Mordasini, C., Burn, R., et al. 2020a, arXiv:2007.05561
 Emshenhuber, A., Mordasini, C., Burn, R., et al. 2020b, arXiv:2007.05562
 Feng, F., Tuomi, M., Jones, H. R. A., et al. 2017, *AJ*, **154**, 135
 Fulton, B. J., Petigura, E. A., Howard, A. W., et al. 2017, *AJ*, **154**, 109
 Gaudi, B. S., Seager, S., Mennesson, B., et al. 2020, arXiv:2001.06683
 Gilbert, G. J., & Fabrycky, D. C. 2020, *AJ*, **159**, 281
 Gray, D. F., & Baliunas, S. L. 1994, *ApJ*, **427**, 1042
 Hall, J. C., & Lockwood, G. W. 2004, *ApJ*, **614**, 942

- Harris, C. R., Millman, K. J., van der Walt, S. J., et al. 2020, *Natur*, 585, 357
- He, M. Y., Ford, E. B., & Ragozzine, D. 2019, *MNRAS*, 490, 4575
- Huang, S.-S. 1959, *PASP*, 71, 421
- Hunter, J. D. 2007, *CSE*, 9, 90
- Kanodia, S., Wolfgang, A., Stefansson, G. K., Ning, B., & Mahadevan, S. 2019, *ApJ*, 882, 38
- Kasper, M., Arsenault, R., Käuffl, U., et al. 2019, *Msng*, 178, 5
- Kervella, P., Arenou, F., Mignard, F., & Thévenin, F. 2019, *A&A*, 623, A72
- Kopparapu, R. K., Ramirez, R., Kasting, J. F., et al. 2013, *ApJ*, 765, 131
- Lagrange, A. M., Bonnefoy, M., Chauvin, G., et al. 2010, *Sci*, 329, 57
- Lawler, S. M., Di Francesco, J., Kennedy, G. M., et al. 2014, *MNRAS*, 444, 2665
- Limbach, M. A., & Turner, E. L. 2015, *PNAS*, 112, 20
- MacGregor, M. A., Lawler, S. M., Wilner, D. J., et al. 2016, *ApJ*, 828, 113
- Macintosh, B., Graham, J. R., Barman, T., et al. 2015, *Sci*, 350, 64
- Mamajek, E. E., & Hillenbrand, L. A. 2008, *ApJ*, 687, 1264
- Mayor, M., Pepe, F., Queloz, D., et al. 2003, *Msng*, 114, 20
- Mazin, B., Artigau, E., Bailey, V., et al. 2019, *BAAS*, 51, 128
- Mulders, G. D., Pascucci, I., Apai, D., & Ciesla, F. J. 2018, *AJ*, 156, 24
- Ning, B., Wolfgang, A., & Ghosh, S. 2018, *ApJ*, 869, 5
- Otegi, J. F., Bouchy, F., & Helled, R. 2020, *A&A*, 634, A43
- Owen, J. E., & Wu, Y. 2017, *ApJ*, 847, 29
- Pascucci, I., Mulders, G. D., & Lopez, E. 2019, *ApJL*, 883, L15
- Pepe, F. A., Cristiani, S., Rebolo Lopez, R., et al. 2010, *Proc. SPIE*, 7735, 77350F
- Plavchan, P., Barclay, T., Gagné, J., et al. 2020, *Natur*, 582, 497
- Quanz, S. 2019, EPSC, 2019, EPSC-DPS2019-327
- Quanz, S. P. 2015, EPSC, 2015, EPSC2015-910
- Santos, N. C., Israelian, G., García López, R. J., et al. 2004, *A&A*, 427, 1085
- Suárez Mascareño, A., Faria, J. P., Figueira, P., et al. 2020, *A&A*, 639, A77
- Teixeira, T. C., Kjeldsen, H., Bedding, T. R., et al. 2009, *A&A*, 494, 237
- The LUVOIR Team 2019, arXiv:1912.06219
- Tuomi, M., Jones, H. R. A., Jenkins, J. S., et al. 2013, *A&A*, 551, A79
- Van Eylen, V., Albrecht, S., Huang, X., et al. 2019, *AJ*, 157, 61
- Virtanen, P., Gommers, R., Oliphant, T. E., et al. 2020, *NatMe*, 17, 261
- Wagner, K. R. 2020, PhD thesis, Univ. Arizona
- Wang, J., Meyer, M., Boss, A., et al. 2019, *BAAS*, 51, 200